NUMERICAL ANALYSIS OF HIGH-SPEED IMPULSIVE (HSI) NOISE OF PZL W3-A "SOKÓŁ" (FALCON) HELICOPTER MAIN ROTOR IN FORWARD FLIGHT

OSKAR SZULC[1], PIOTR DOERFFER[1], FERNANDO TEJERO[1], JERZY ŻÓŁTAK[2] AND JACEK MAŁECKI[3]

*[1]Institute of Fluid-Flow Machinery, Polish Academy of Sciences
Fiszera 14, 80-231 Gdansk, Poland*

*[2]Institute of Aviation
Al. Krakowska 110/114, 02-256 Warszawa, Poland*

*[3]PZL-Świdnik S. A., AugustaWestland
Al. Lotników Polskich 1, 21-045 Świdnik, Poland*

Abstract: The paper presents the results of a numerical simulation of the flow and acoustic field generated by the PZL W3-A "Sokół" (Falcon) helicopter main rotor in high-speed forward flight conditions based on the URANS approach and the chimera overlapping grids technique. A refined CFD model (40+ million of control volumes, 600+ blocks chimera mesh) was designed to resolve the flow-field together with the low-frequency content of the acoustic pressure spectrum in the near-field of the rotor blades to allow high-speed impulsive (HSI) noise prediction. Detailed 3D data was recorded for one rotor revolution (approx. 3 TB) allowing exceptional insight into the physical mechanisms initiating the occurrence and development of the HSI noise phenomenon.

Keywords: aerodynamics, CFD, forward flight, helicopter rotor, HSI noise, shock wave

1. Introduction

PZL W3 "Sokół" (Falcon) is a Polish, medium-size, twin-engine, multipurpose helicopter constructed by PZL-Świdnik, now a member of the British-Italian AugustaWestland company (Figure 1). This first helicopter fully designed and serially produced in Poland has been continuously in service since 1987. The original main rotor design has served for more than 25 years and is still operating in hundreds of machines sold all over the world. The increasing significance of

the fuel consumption and noise emission restrictions forces the design of an improved version of the helicopter with enhanced performance and reduced fly-over noise. A completely new, 4-bladed main rotor (based on the ILH family of profiles recently developed at the Instytut Lotnictwa in Warsaw [1]) for the modernized W3-A "Sokół" (Falcon) helicopter is designed and manufactured by the Instytut Lotnictwa and PZL-Świdnik, verified experimentally through scale model wind tunnel tests by the Instytut Lotnictwa and tested numerically by the Institute of Fluid-Flow Machinery in Gdansk.

Figure 1. PZL W3-A "Sokół" (Falcon) of the Polish Tatra Volunteer Search and Rescue

The unrestricted part of the work (described in the article) contains aerodynamic and aero-acoustic results of a numerical simulation of the original 4-bladed NACA rotor in high-speed forward flight. Over the duration of the project detailed simulations of both NACA and ILH rotors were performed and compared for different low- and high-speed forward flight conditions. The numerical results suggest that the new, ILH rotor is more efficient and emits less noise in flight compared to the older NACA design, but so far the data could not be published due to the confidentiality issues. Hence, the aerodynamic results of the high-speed case will be compared with very limited flight-test data, while for the acoustic part it is only the CFD results that are available, both for the original NACA rotor only.

## 2. Physical and numerical modeling

2.1. FLOWer code from DLR

The present investigation was carried out with the FLOWer solver from DLR [2]. It is a modern, parallel, block-structured, cell-centered code solving Favre-averaged Navier-Stokes equations with various turbulence models. The ROT/CHIMERA version of the code allows using the chimera overlapping grids technique and moving meshes. From various turbulence closures implemented in FLOWer, a two-equation, low-Reynolds k-ω turbulence model of LEA (Linear Explicit Algebraic Stress Model) was chosen [3]. The numerical algorithm uses a semi-discrete approach, utilizing a 2nd order finite-volume formulation for the spatial discretization and a 2nd order implicit dual-time-stepping (with explicit 5-stage Runge-Kutta) method for integration in time. A scalar artificial dissipation model of Jameson is implemented to damp numerical oscillations. A time step equal to the time needed for a rotation by $0.25°$ of azimuth (*i.e.* 1440 time steps

per period of rotation) and a CFL number ≤ 10.0 for the internal R-K stages was set for the dual time-stepping scheme. At each physical time step the density residual gained a drop of 3.0 orders of magnitude within several iterations, which proved to be sufficient to obtain an accurate, unsteady flow-field around the rotor.

2.2. Rotor geometry

The first approximation is to abandon the influence of the fuselage and the tail rotor and to isolate the main rotor blades. The elastic deformations due to the air-loads are neglected in the overall picture as well. The rotor of the PZL W3-A "Sokół" (Falcon) helicopter consists of 4 blades (based on the NACA 23012M airfoil) having a radius of $R = 7.85$ m and linearly twisted from $0°$ at the root up to $-12°$ at the tip location (Figure 2). Apart from the root area, the trimming tabs and the tip region, the chord is equal to $c = 0.44$ m. The rotor rotates in the clockwise direction (as seen from above). In forward flight the rotor blades not only rotate around the azimuth, but also pitch and flap (the lead-lag motion is not considered here). The azimuth angle is assumed to be $0°$ for the first blade when it is pointing in the direction opposite to the flight direction. In forward flight the shaft normal plane is additionally inclined to the flight direction (inflow) at a constant angle.
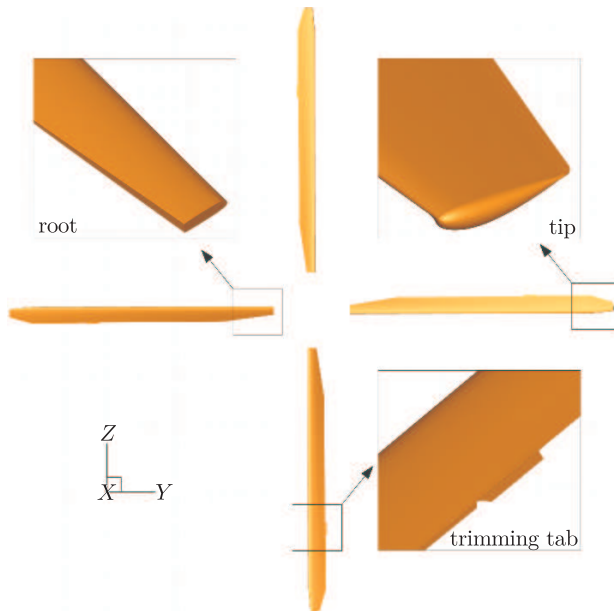

Figure 2. Numerical model of the main rotor of PZL W3-A "Sokół" (Falcon)

2.3. Chimera component grids

The main idea of the chimera technique implemented in the FLOWer code is to easily generate grids for complex configurations by decomposing them into simple, independent parts [4]. The only limitation is that all component meshes

should overlap each other to allow inter-grid communication. In case of rotors in forward flight the chimera overlapping grids technique allows easy control of the rigid motion of the blades (translation, rotation, pitch and flap) preventing any grid deformation. The component overlapped grids for the PZL W3-A "Sokół" (Falcon) helicopter rotor were generated using a script based approach and the Interactive Grid Generator (IGG) from Numeca International allowing semi-automatic meshing. Three component grids created for a single rotor blade (root, center and tip areas) are placed within the background Cartesian mesh. The remaining three blades are generated automatically by the FLOWer solver.

The Cartesian background grid is designed as a cuboid with the dimensions of $16.4\,R \times 18.2\,R \times 18.2\,R$. Consequently, the far-field surface is located at least $8.0\,R$ away from the rotor in every direction (Figure 3). 32 computational blocks contain $10.4 \cdot 10^6$ volumes (25% of the total number of cells). The core of the background grid surrounding the rotor blades is divided into 4 computational blocks ($240 \times 240 \times 48$, $2.8 \cdot 10^6$ volumes) extending beyond the blade tip to $1.1\,R$ and reaching $\pm 0.22\,R$ above and below the rotor plane (Figure 4). A uniform Cartesian grid (dimensions of volumes: $0.16\,c \times 0.16\,c \times 0.16\,c$) located in this refined area constitutes an "acoustic box" designed to support propagation of the acoustic pressure waves resolved in space up to $950\,\mathrm{Hz}$ (5 points per wavelength) and detected up to $2380\,\mathrm{Hz}$ (2 points per wavelength). Away from the rotor the grid spacing is more relaxed. The background grid component undergoes translation with forward flight velocity and a constant tilt by a shaft angle.
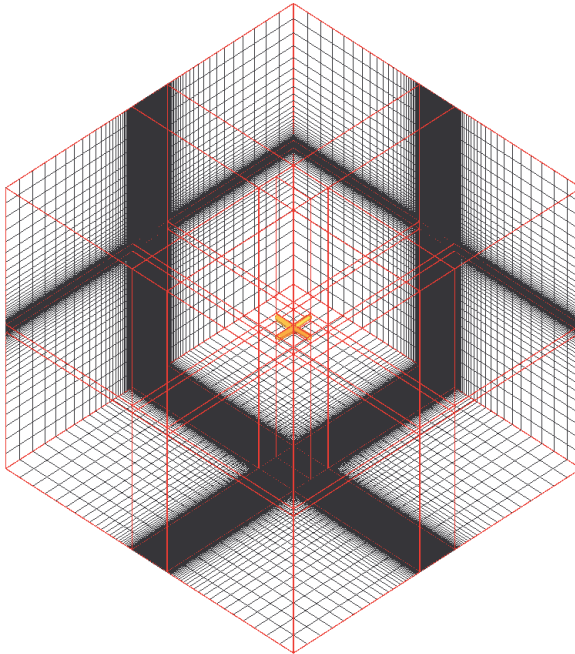


Figure 3. Background component grid
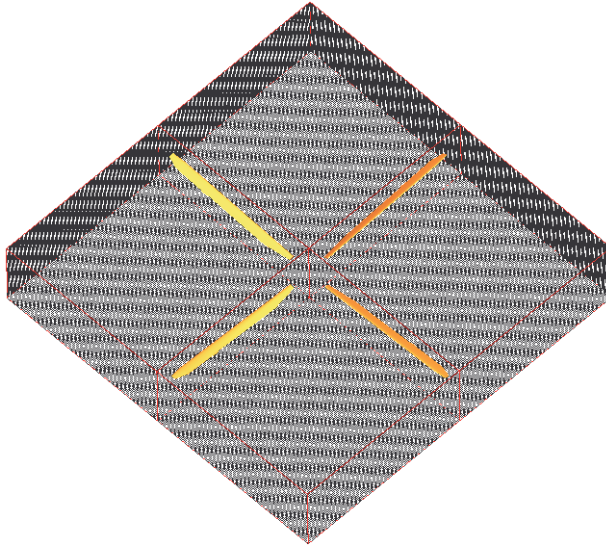
Figure 4. Acoustic box

The region of the blade root (Figure 5) is meshed using an O-type grid in stream-wise and H-type grid in crosswise directions. It spans from the surface for 2 chord lengths (0.88 m) in the normal direction and 1.5 chords (0.66 m) in the radial direction. It consists of 13 blocks and $1.2 \cdot 10^6$ volumes per blade. The majority of the blade is covered by the center (Figure 6) chimera component grid of a C-type in streamwise and H-type in crosswise directions. It spans from the surface for 2 chord lengths (0.88 m) in the normal direction and consists of 118 blocks and $5.3 \cdot 10^6$ volumes per blade. The close-up at the bottom left corner
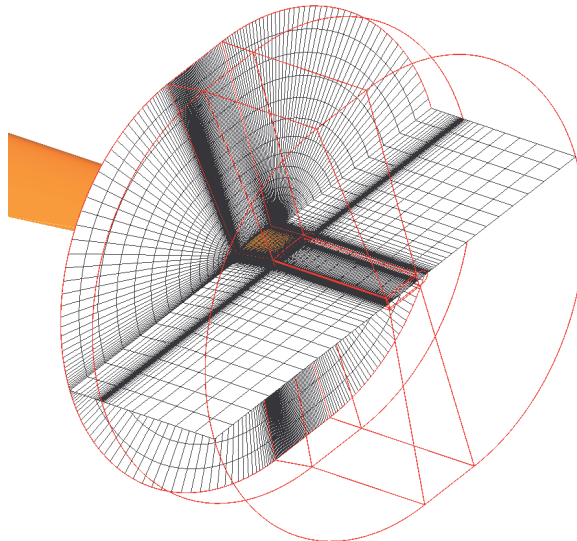
Figure 5. Blade root component grid
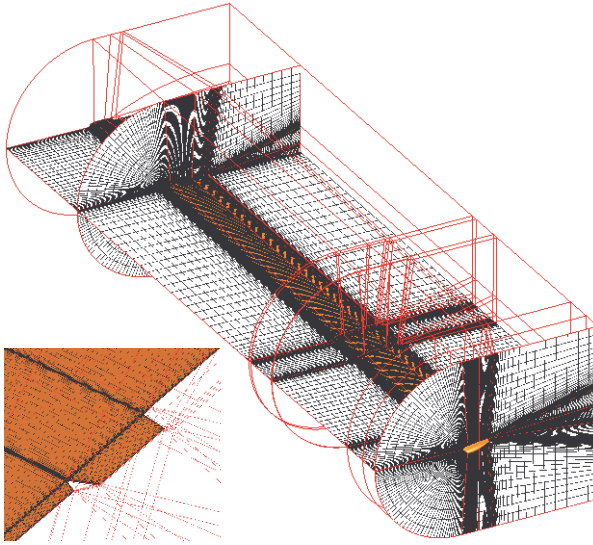
Figure 6. Blade center component grid
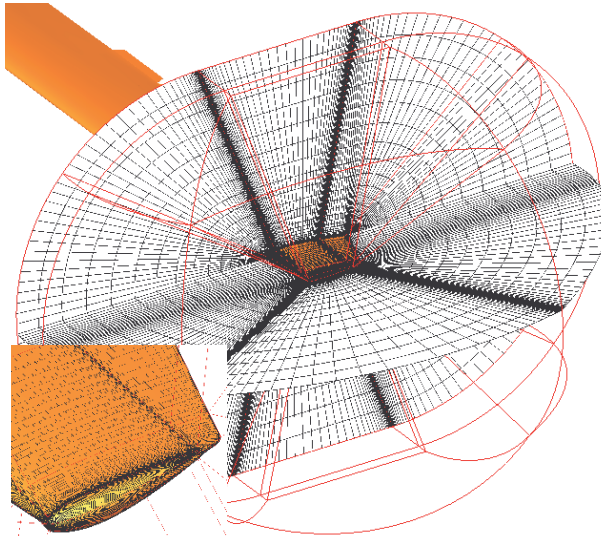
Figure 7. Blade tip component grid

of Figure 6 reveals the geometrical complexity of the surface mesh and block topology near the trimming tab located at the trailing edge of the blade (area depicted in Figure 2 as "trimming tab"). The last component grid covers the area of the blade tip (Figure 7). Due to a rounded tip shape an O-type grid is applied in streamwise and crosswise directions. It spans from the surface for 2 chord lengths (0.88 m) in the normal direction and consist of 19 blocks and $1.1 \cdot 10^6$ volumes per blade. The close-up at the bottom left corner of Figure 7 presents the rounded tip surface mesh in more details (area depicted in Figure 2 as "tip"). The root,

center and tip components undergo all the prescribed motions: the translation with forward flight velocity, the rotation around the azimuth, a constant tilt by a shaft angle, the unsteady pitch and flap. A complete set of meshes consists of 632 blocks and $40.6 \cdot 10^6$ control volumes. The blade component grids (root – green, center – red and tip – blue color) of the first blade are placed in the background grid (Figure 8). The remaining three blades are set-up and managed by the FLOWer solver.
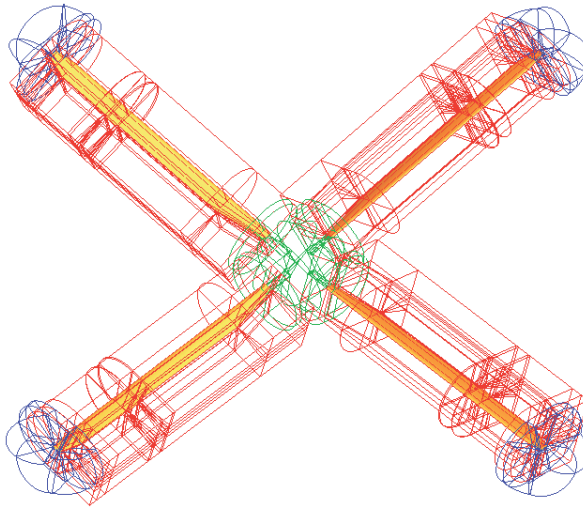

Figure 8. Rotor chimera grid topology

2.4. Flight test conditions

The high-speed flight test (266 km/h) of the PZL W3-A "Sokół" (Falcon) helicopter was performed at 931 m above the sea level in the temperature of 5.2°C. The rotor operated at 28 rad/s with the tip Mach number of 0.66, the tip Reynolds number of $6.3 \cdot 10^6$, the forward flight Mach number of 0.22 and the forward flight Reynolds number of $2.1 \cdot 10^6$ (the advance ratio of 0.34). During the flight test the instantaneous values of rotor control angles were recorded (pitching, flapping and shaft tilt according to the flight direction) and applied in the simulation (see details in [5]).

3. Validation of the method

3.1. Caradonna-Tung model helicopter rotor in high-speed hover

The aerodynamic validation of the FLOWer solver applied to rotorcraft flows against the experimental data was based on a famous NASA test case from 1981 of the Caradonna-Tung (C-T), two-bladed model helicopter rotor in high-speed, transonic hover conditions, operating with a tip Mach number of 0.877 and collective of 8° [6]. A Q-criterion visualization (colored by the vorticity magnitude)

of the rotor flow-field and wake was extracted from the FLOWer numerical solution based on a structured grid and Spalart-Allmaras (SA) turbulence model (Figure 9). On the other hand, an exemplary pressure coefficient distribution c_p obtained using again the FLOWer code and the chimera overlapping grids technique (SA turbulence closure) is compared in Figure 10 with the experimental data measured at the chordwise cross-section of the blade $r/R = 0.89$ (more information in [7–9]). The solutions presented in Figures 9 and 10, based on the block-structured and chimera grids are of equal quality (compared with the experimental data) as the previous numerical results obtained using two other CFD codes: SPARC from the University of Karlsruhe (Germany) [7, 10–12] and Fine/Turbo from Numeca Int. (Belgium) [7]. The FLOWer results obtained for a hovering C-T rotor using the chimera set-up and LEA k-ω turbulence model
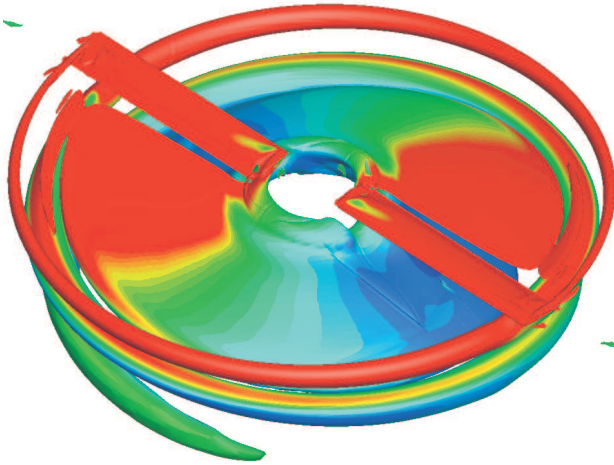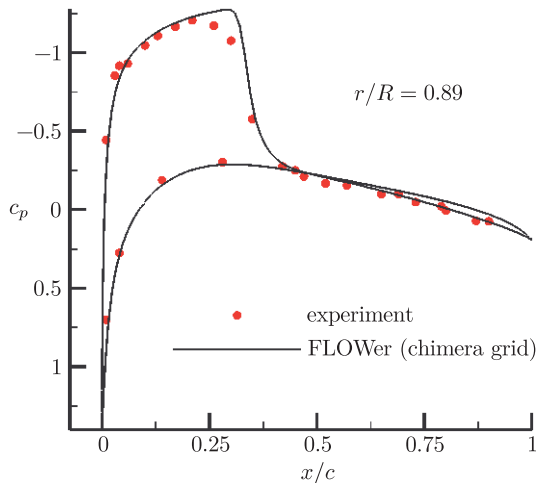

Figure 9. Caradonna-Tung rotor wake

Figure 10. Pressure coefficient c_p

(a combination applied for the PZL W3-A "Sokół" (Falcon) and the AH-1G Cobra helicopter main rotor forward-flight simulations) are validated as well, but presented with more details in [8, 9, 13].

3.2. *AH-1G Cobra helicopter rotor in high-speed forward flight*

The aerodynamic validation of the forward flight capabilities of the FLOWer code and chimera overlapping grids technique using the LEA k-ω turbulence model was performed against the flight test data gathered by Cross J.L. and Watts M.E. at NASA in 1981 for the AH-1G Cobra helicopter equipped with a 2-bladed, OLS main rotor in low-, medium- and high-speed flights [14]. In high-speed forward flight (290 km/h) the rotor operated with the tip Mach number of 0.64 and forward flight Mach number of 0.24 (advance ratio of 0.38). During the flight test the instantaneous values of thrust coefficient C_T and pressure coefficient c_p distributions at several cross-sections of the blade were measured. The recorded rotor control angles (pitching, flapping and shaft inclination regarding the flight direction) were applied in the simulation as well. The Q-criterion (colored by the vorticity magnitude) visualization of the flow-field of the rotor at the azimuthal position of 80° is extracted from the FLOWer numerical solution (Figure 11). Serving as an example the normal force coefficient c_n vs. azimuth ψ and chordwise pressure coefficient c_p distribution are compared with the experimental data measured at $r/R = 0.86$ (more details in [8, 9]). The calculated averaged thrust coefficient C_T is overpredicted by 20%. This leads to the conclusion of a significant influence of the modeling simplifications related to the rigid blade assumption (no flexibility), lack of the fuselage and tail rotor or absence of the main rotor trimming. Still, the data may be used for a comparative study of rotors in terms of the aerodynamic and aero-acoustic performance. Contrary to the low-speed data, the presented CFD results for the high-speed flight test are unique in terms of the literature survey.

4. Numerical results

4.1. *Flow-field of the PZL W3-A "Sokół" (Falcon) helicopter main rotor in high-speed forward flight*

The flow-field around the PZL W3-A "Sokół" (Falcon) helicopter main rotor in high-speed forward flight is visualized by an iso-surface of the Q-criterion (colored by the vorticity magnitude) in Figure 12. The blade tip and trimming tabs create strong vortices that interact with the blades leading to the perpendicular and parallel blade-vortex interactions. Due to high relative inflow velocity at the advancing side large areas of the supersonic flow emerge, terminated by shock waves, having a significant impact on the level of the generated high-speed impulsive (HSI) noise. The rotor thrust C_T and power C_P coefficients fluctuate in time with the mean values equal to: $C_T = 0.00666$ and $C_P = 0.000705$. The mean component of the force acting against the weight of the helicopter is equal to 7130 kg and the mean power is equal to 2200 HP. It is worth to mention that the
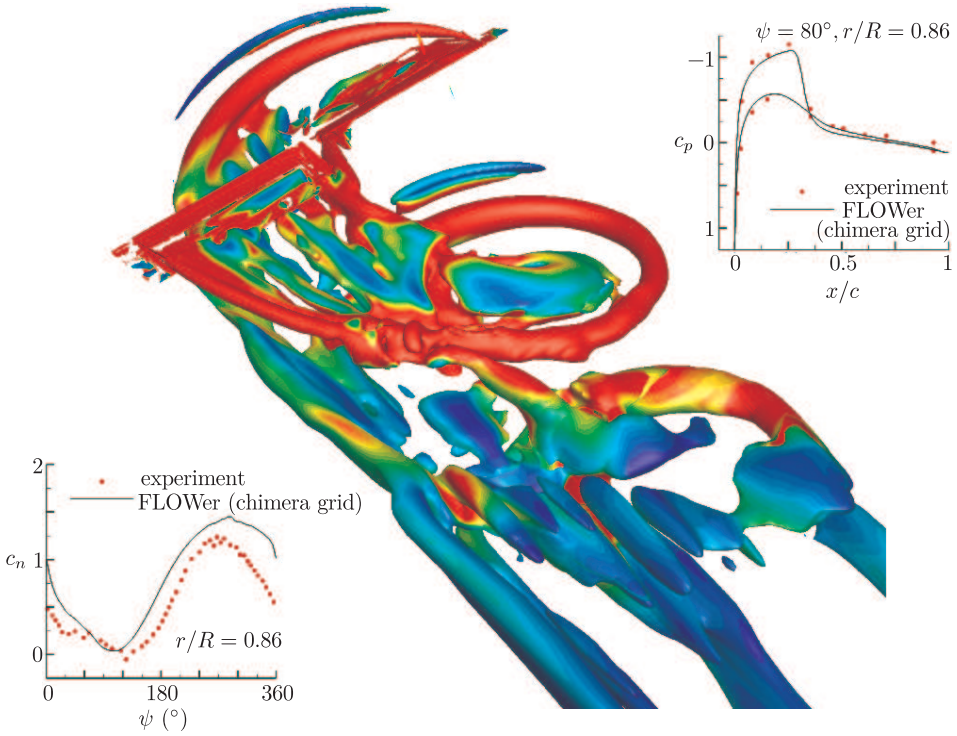
Figure 11. AH-1G Cobra rotor wake, pressure c_p and normal force c_n coefficients
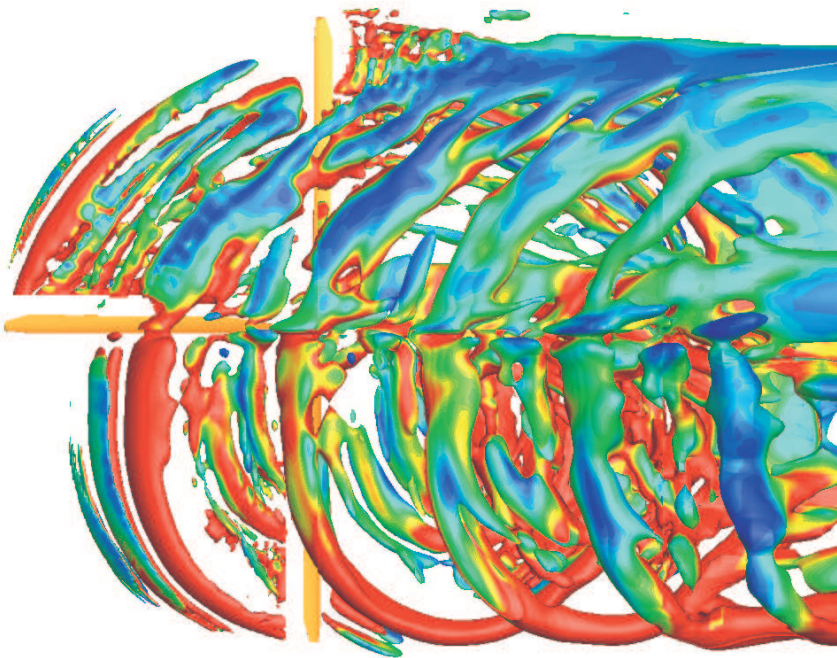

Figure 12. PZL W3-A "Sokół" (Falcon) helicopter rotor wake (as seen from below)

PZL W3-A "Sokół" (Falcon) helicopter had a take-off weight of 6100 kg (minus 150 kg of the consumed fuel) and was equipped with engines of the total power of 1800 HP. The numerical simulation of the flow past the isolated rotor of the PZL W3-A "Sokół" (Falcon) helicopter in high-speed forward flight leads to an overprediction of the mean thrust and power by ∼20% compared to the flight test data of a complete helicopter (more details in [5]). It is worth mentioning that very similar deviations in the aerodynamic performance have been presented in subsection 3.2 devoted to the AH-1G Cobra helicopter main rotor in high-speed flight.

4.2. Acoustic field of the PZL W3-A "Sokół" (Falcon) helicopter main rotor in high-speed forward flight

The acoustic post-processing of the flow-field of the PZL W3-A "Sokół" (Falcon) helicopter main rotor in high-speed forward flight is based on an analysis of a large set of output 3d data files (3 TB) containing density, pressure and velocity components as well as turbulent quantities. The data is recorded for one rotation period of the rotor every 1° of azimuth (the CFD simulation is progressed in time with 0.25° time-step) while keeping the space resolution unmodified. It is worth mentioning that the "acoustic box" uniform grid refinement of the volume enclosing the rotor blades supports propagation of the acoustic pressure fluctuations up to a frequency of 950 Hz (5 points per wavelength) and detection up to a frequency of 2380 Hz (2 points per wavelength). Outside of the "acoustic box" the resolution of the grid decreases, leading to a strong suppression of the acoustic waves. Since the rotorcraft high-speed impulsive noise phenomenon is low-frequency dominated and emitted mostly in the rotor plane the model constitutes a good approximation of the generation and near-field propagation of the acoustic signals [15].

An example "snapshot" of the instantaneous acoustic pressure field at a plane perpendicular to the shaft and located 0.35 m above the rotor hub is presented in Figure 13. The pressure fluctuation scale is limited to a range from -100 Pa to 100 Pa in order to distinct weak acoustic waves from a very intense background. Due to the coning and flapping motion the root and inner parts of the blades are located below, while the outer parts and tips are positioned above the chosen plane. A particularly strong HSI pressure impulse (~ 140 dB) is generated by the advancing blade at 90° of azimuth and transmitted in the direction forward of the helicopter (marked as "HSI noise" in Figure 13). To quantify the aerodynamic noise of the rotor the overall sound pressure level *OASPL* [dB] measure is presented in Figure 14. The averaging process of the root mean square (rms) of the acoustic pressure amplitude is based on the interpolation of the value onto a uniform, 2d planar grid (2140×2140, $4.6 \cdot 10^6$ cells, resolution of $0.1c$) being perpendicular to the shaft and located also 0.35 m above the rotor hub. Due to high advance ratio of 0.34 the *OASPL* map is highly asymmetrical with higher values shifted to the advancing side of the rotor. The maximum value of the *OASPL* recorded in the rotor disc at this plane is extremely high and equal
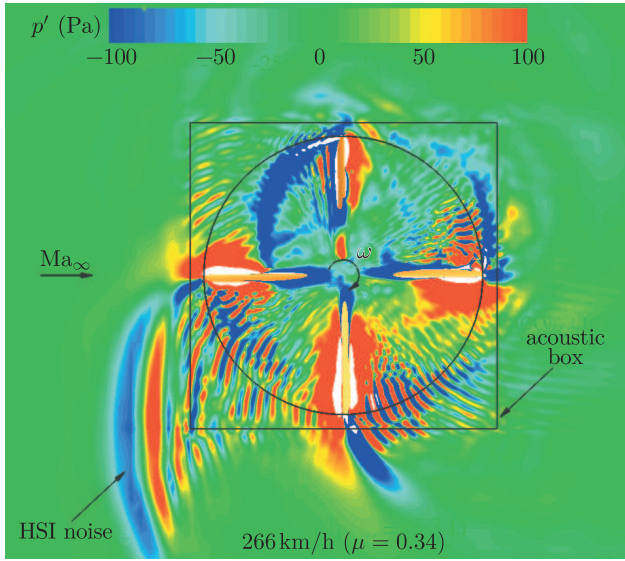
Figure 13. Instantaneous acoustic pressure
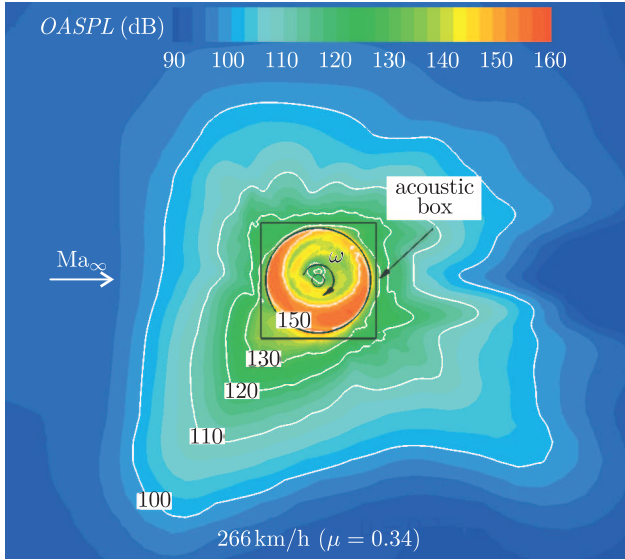
Figure 14. Overall sound pressure level

to 158 dB, but still lower than the maximum value in the whole volume (161 dB) located at the plane that is crossing the advancing blade tip at 90° of azimuth (0.58 m above the rotor hub). The maximum noise level is decreasing to 145 dB when probing the pressure farther away from the rotor at a circle with a radius of 8.635 m (inscribed in the "acoustic box" at the same plane located 0.58 m above the rotor hub). Already at 5 m from the tip of the advancing blade at 90° of azimuth the noise level drops to ∼120 dB.

The HSI noise phenomenon is strongly dependent on a maximum inflow Mach number present at the advancing blade at 90° of azimuth called advancing tip Mach number Ma_{AT} [16]. The shape and amplitude of the acoustic pulse are changing non-linearly with increasing Ma_{AT}. Below a critical value (called the delocalization Mach number) the smooth acoustic waveform is symmetrical (elliptic). Above and at the delocalization Mach number the pulse changes dramatically into a shock waveform (hyperbolic). For the UH-1H helicopter rotor (2-bladed, rectangular and untwisted NACA 0012) operating in non-lifting, hovering conditions the delocalization is initiated between $Ma_{AT} = 0.88$ and 0.90 [17]. For more advanced rotors (in terms of airfoil or blade tip planform, i.e. swept, tapered or thinned) this border is shifted to even higher values of $Ma_{AT} > 0.92$. In a rotating frame of reference the described transition occurs when a local supersonic pocket (relative Mach number $Ma_r > 1.0$) located at the blade tip develops a connection with the non-linear sonic cylinder (surface of a relative Mach number $Ma_r = 1.0$). For this reason, the visualization of the Ma_r is of great importance in a study of the HSI noise and is presented for the PZL W3-A "Sokół" (Falcon) helicopter rotor in Figure 15. In the analyzed high-speed flight with $Ma_{AT} = 0.88$ the supersonic area ($Ma_r > 1.0$) located near the tip of the advancing blade is not connected with a non-liner sonic cylinder ($Ma_r = 1$) leading to a HSI noise phenomenon far below delocalization.
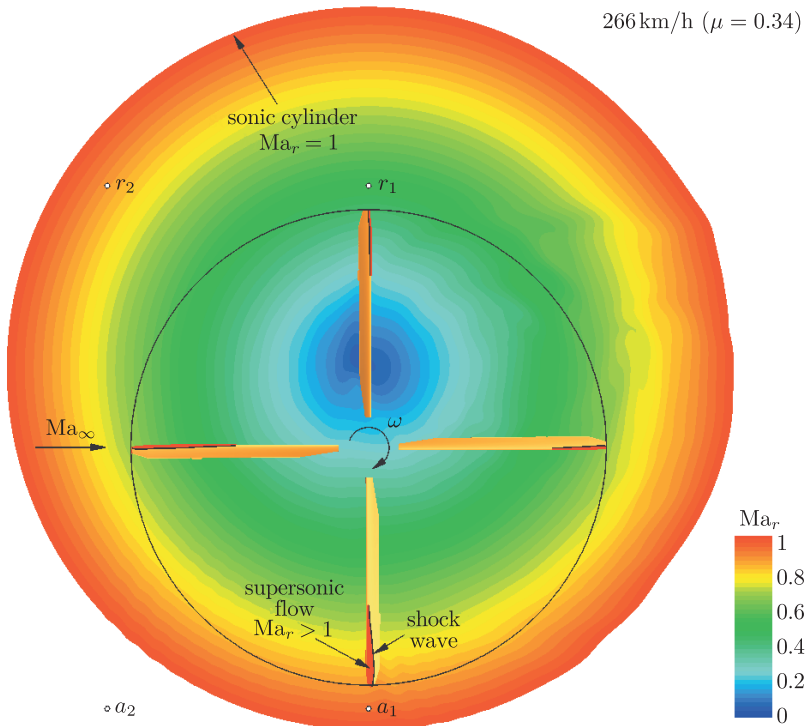

Figure 15. Relative Mach number Ma_r

Although the shock wave is not delocalized, a very intense acoustic pressure pulse is generated by the advancing blade and emitted forward along the direction of the helicopter flight. As an example, pressure signals recorded at 4 points a_1, r_1, a_2 and r_2 (two at the advancing and two at the retreating side – see Figure 15) at a plane located 0.35 m above the rotor hub are presented in Figure 16. The first extraction point a_1 is positioned at the advancing side at the azimuth of 90° and 8.635 m $(r/R = 1.1)$ from the rotation axis (on the outer edge of the "'acoustic box"). The corresponding r_1 point is located at the retreating side at the azimuth of 270° with the same distance from the rotor axis. The third point a_2 is positioned at the advancing side at the azimuth of 135° and 12.212 m $(r/R = 1.556)$ from the rotation axis (at the bottom left corner of the "acoustic box"). The corresponding r_2 point is located at the retreating side at the azimuth of 225° with the same distance from the rotor axis. At the blade passing frequency of 17.8 Hz a large pressure peak is visible with an amplitude of more than 1 kPa at point a_1 (source) resulting in the overall sound pressure level (*OASPL*) of 145 dB. At the same time the amplitude of the pressure peak at point r_1 stays below 100 Pa with the *OASPL* of 126 dB. In the area of the near-field propagation at point a_2 the amplitude is still
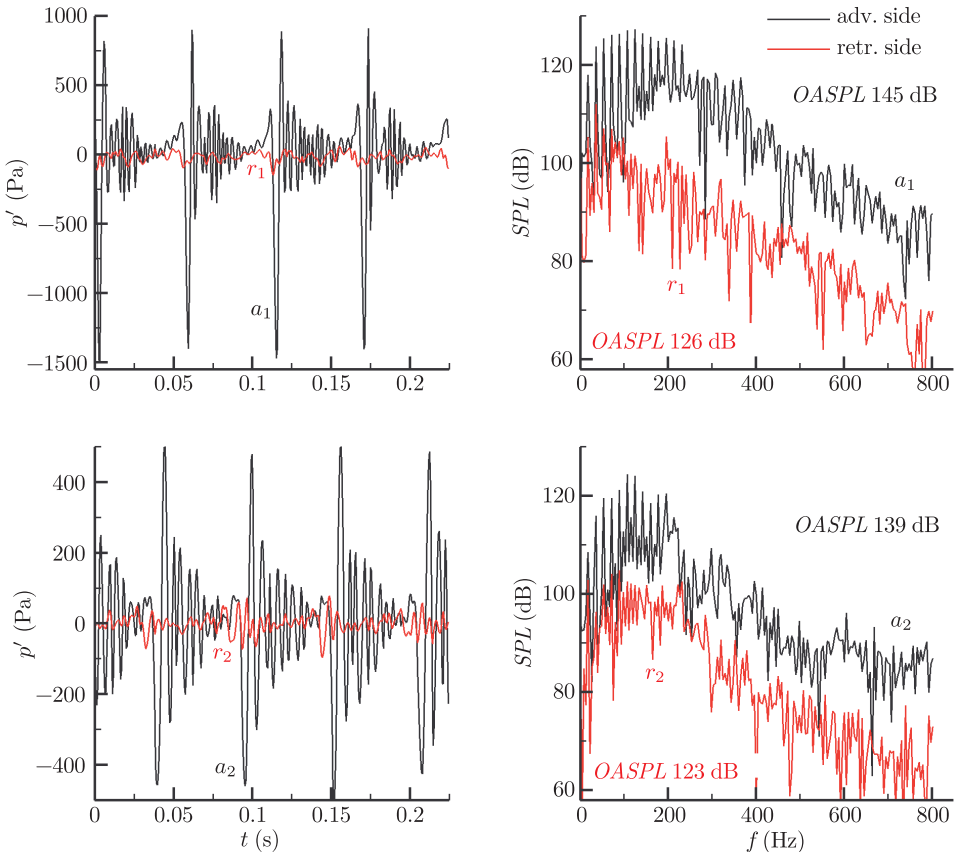

Figure 16. Acoustic pressure p' and sound pressure level *SPL* spectra

large and equal to 500 Pa (*OASPL* of 139 dB). On the other hand, at the retreating side point r_2 the amplitude is limited to 90 Pa and *OASPL* of 123 dB. Both spectra recorded at the advancing side points a_1 and a_2 of the sound pressure level (*SPL*) are dominated by low-frequency content with a maximum energy located between 20 Hz and 240 Hz. The corresponding points r_1 and r_2 at the retreating side of the rotor are dominated by low frequencies as well. The "spikes" visible in Figure 16 correspond to the harmonics of the blade passing frequency. The shape of the presented pressure pulses and *OASPL* spectra are in-line with the experimental observations and flight test data that can be found in the literature (*e.g.* [15, 17]).

5. Conclusions

A computational model based on the FLOWer solver, the URANS approach and the chimera overlapping grids technique was validated proving its ability to predict a complex flow-field of the helicopter rotor in high-speed, transonic hover and forward-flight conditions. Due to a specially prepared background grid (i.e. inclusion of the "acoustic box" refinement) the HSI noise phenomenon was analyzed together with the flow-field in a single numerical simulation resolving not only the area of the acoustic sources, but the near-field propagation as well. A comparative, aero-acoustic study of a well established rotor of the PZL W3-A "Sokół" (Falcon) helicopter with a completely new design based on the ILH family of airfoil sections was successful, but due to the confidentiality issues has not been presented in the article. The methodology described in the article proved to be very advantageous in judging the HSI noise generated by both rotors (NACA and ILH) at the design level of a modernized version of the PZL W3-A "Sokół" (Falcon) helicopter.

Acknowledgements

References

[1] Kania W and Stalewski W 2000 *Development of new generation main and tail rotors blade airfoils, Proceedings of the 22nd Congress of the International Council of the Aeronautical Sciences (ICAS)*, 181.1

[2] Rossow C-C, Kroll N and Schwamborn D 2006 *The MEGAFLOW project – numerical flow simulation for aircraft, Progress in Industrial Mathematics at ECMI 2004*, Di Bucchianico A, Mattheij R M M and Peletier M A (editors), Springer, **8** 3

[3] Rung T, Lübcke H, Franke M, Xue L, Thiele F and Fu S 1999 *Assessment of explicit algebraic stress models in transonic flows, Proceedings of the 4th International Symposium on Engineering Turbulence Modelling and Measurements* 659

[4] Schwarz T 2005 *The overlapping grid technique for the time accurate simulation of rotorcraft flows, Proceedings of the 31st European Rotorcraft Forum* 789

[5] Szulc O, Doerffer P, Żółtak J and Małecki J 2013 *TASK Quarterly* **17** (1–2) 43

[6] Caradonna F X and Tung C 1981 *Experimental and analytical studies of a model helicopter rotor in hover*, *NASA Technical Memorandum* **81232**

[7] Doerffer P, Szulc O, Tejero Embuena F L and Martinez Suarez J 2014 *Aerodynamic and aero-acoustic analysis of helicopter rotor blades in hover, eScience on Distributed Computing Infrastructure. Achievements of PLGrid Plus Domain-Specific Services and Tools*, Bubak M, Kitowski J and Wiatr K (editors), Springer, **8** 429

[8] Tejero Embuena F L, Doerffer P and Szulc O 2014 *Journal of Physics: Conference Series* **530** (1) 12067

[9] Tejero Embuena F L, Doerffer P and Szulc O 2015 *Application of passive flow control device on helicopter rotor blades, Journal of the American Helicopter Society* (accepted)

[10] Doerffer P and Szulc O 2008 *TASK Quarterly* **12** (3) 227

[11] Doerffer P and Szulc O 2010 *TASK Quarterly* **14** (3) 297

[12] Doerffer P and Szulc O 2011 *International Journal of Engineering Systems Modelling and Simulation* **3** (1–2) 64

[13] Tejero Embuena F L, Doerffer P, Flaszyński P and Szulc O 2014 *Numerical investigation of rod vortex generators on hovering helicopter rotor blade*, Proceedings of the 6th European Conference on Computational Fluid Mechanics

[14] Cross J L and Watts M E 1988 *Tip Aerodynamics and Acoustics Test. A report and data survey, NASA Reference Publication* **1179**

[15] Schmitz F H and Yu Y H 1983 *Helicopter impulsive noise: theoretical and experimental status, NASA Technical Memorandum* **84390**

[16] Yu Y H, Park S H, Lee J W and Byun Y H 2007 *Journal of the Korean Physical Society* **51**, S52

[17] Purcell T W 1988 *CFD and transonic helicopter sound, Proceedings of the 14*[th] *European Rotorcraft Forum*